International Journal of Environmental Sciences
ISSN: 2229-7359
Vol. 11 No. 18s, 2025
https://theaspd.com/index.php

Sustainable Photocatalytic Degradation Of Phenol Using Iron-Based Bead Catalyst

Muhammad Farhan Hanafi [a,b*], Muhamad Hafiffy Kamaruddin [a], Diyana Faziha Mohamad [a], Norzahir Sapawe [a*]
[a]Universiti Kuala Lumpur Branch Campus Malaysian Institute of Chemical and Bioengineering Technology (UniKL MICET), Lot 1988 Vendor City, Taboh Naning, 78000 Alor Gajah, Melaka, Malaysia
[b]Department of Chemical Engineering and Energy Sustainability, Faculty of Engineering, Universiti Malaysia Sarawak (UNIMAS), 94300 Kota Samarahan, Sarawak, Malaysia

[*]Corresponding author – norzahir@unikl.edu.my, hmfarhan@unimas.my

ABSTRACT
The increasing industrial reliance on phenol has led to a significant rise in phenolic pollution, necessitating effective and sustainable treatment methods. In this study, a nanocomposite iron bead catalyst was synthesized and evaluated for the photocatalytic degradation of phenol in aqueous solution. The degradation performance was assessed under varying conditions, including pH levels (3, 5, 7, 8, 9, and 11), catalyst dosages (10, 20, 30, 40, and 50 g/L), and initial phenol concentrations (10, 20, 30, 40, 70, and 100 ppm). UV-Vis spectrophotometry was employed to determine phenol removal efficiency over a reaction time of 3 hours. The functional groups and structural features of the iron bead catalyst were characterized using FTIR spectroscopy, revealing a strong absorption band at 570.36 cm^{-1} corresponding to the Fe–O stretching vibration in Fe_3O_4, confirming the presence of magnetite nanoparticles. Additional bands between 500–700 cm^{-1} were attributed to Fe–O bonds in iron oxide structures. The optimal degradation condition was achieved at pH 3, with a catalyst dosage of 40 g/L and an initial phenol concentration of 10 ppm, resulting in a 95% removal efficiency at room temperature within 3 hours. The simple and time-efficient synthesis of the iron bead catalyst, coupled with its excellent degradation performance, demonstrates its potential as a viable alternative to conventional phenol removal methods.
Keywords : *Iron bead catalyst, phenol, photocatalytic degradation, visible light irradiation, wastewater treatment*

1. INTRODUCTION

Environmental pollution, particularly water contamination from industrial activities, has become a major global concern. Industrial and medical effluents often contain hazardous organic and inorganic compounds, including heavy metals, dyes, and aromatic compounds. Among these pollutants, phenol and its derivatives are especially toxic and pose serious risks to aquatic life and human health even at low concentrations [1,2]. Phenol is a common aromatic pollutant generated by a wide range of industries, including petrochemical, pharmaceuticals, dyes, pesticides, plastics, resins, pulp and paper, and textile manufacturing [3,4]. Because of its toxicity, resistance to biodegradation, and persistence in the environment, phenol is listed as a priority pollutant by the United States Environmental Protection Agency (US EPA). According to the World Health Organization (WHO), the maximum allowable concentration of phenol in drinking water is 1 µg/L [5]. However, phenol concentrations in industrial wastewater have been reported to reach levels as high as 2000 mg/L, far exceeding the safe limit [2]. The release of phenolic wastewater into natural water bodies without proper treatment can cause severe ecological imbalance and pose direct threats to human and animal health. Hence, efficient and sustainable remediation strategies are urgently needed to address this issue.

Traditionally, phenol removal has relied on methods such as biological treatment, chemical oxidation, coagulation, and adsorption. Although these methods can be effective, they are often limited by high operational costs, long treatment times, and the potential generation of secondary pollutants [6,7]. Among emerging approaches, advanced oxidation processes (AOPs)—notably photocatalytic degradation—have shown great potential due to their ability to degrade phenol into less harmful compounds through the generation of reactive oxygen species under light irradiation. Photocatalysis is an environmentally friendly and energy-efficient technique, especially when combined with heterogeneous catalysts, which are easily separable and reusable. In recent years, iron-based catalysts have gained attention for their effectiveness in degrading organic pollutants, thanks to their strong redox potential, natural

abundance, low toxicity, and low cost [8]. To enhance catalyst recovery and stability, iron nanoparticles can be immobilized into polymeric matrices to form iron-based bead catalysts, offering improved surface area, active site accessibility, and ease of reuse.

Sodium alginate (SA), a biodegradable and non-toxic polysaccharide extracted from brown seaweed, is widely used as a matrix material for encapsulating active substances. When cross-linked with calcium chloride ($CaCl_2$), it forms stable hydrogel beads with a three-dimensional network that can encapsulate iron nanoparticles efficiently [9]. The interaction between calcium ions and the guluronic acid blocks of alginate enables the formation of beads with good mechanical properties and water stability, making them suitable for wastewater treatment applications [10]. Several techniques, including sol-gel encapsulation, impregnation, and coating, have been employed to prepare nanocomposite beads. Among these, the sol-gel method stands out for its simplicity, scalability, and environmentally benign nature. In this study, iron-based nanocomposite beads (Fe-beads) were synthesized using sodium alginate and calcium chloride via the sol-gel technique to evaluate their photocatalytic performance in phenol degradation.

This research emphasizes the sustainable use of iron-based bead catalysts for photocatalytic phenol degradation, offering a low-cost, reusable, and green alternative to conventional treatment technologies [7,11,12]. By optimizing critical parameters such as pH, catalyst dosage, and initial phenol concentration, this study aims to provide valuable insight into the practical application of iron-based beads for wastewater treatment, contributing toward cleaner production and circular economy initiatives.

2. MATERIALS AND METHODS

2.1 Materials

The primary chemicals used in this study include iron (Fe) powder, sodium alginate (SA, $C_6H_9NaO_7$), and calcium chloride ($CaCl_2$), all procured from Bendosen. These materials are essential for fabricating the iron-based beads, where SA serves as the encapsulating polymer, calcium chloride acts as the crosslinking agent, and iron functions as the active photocatalyst. Hydrochloric acid (HCl, 1.0 M) and sodium hydroxide (NaOH, 1.0 M), purchased from QReC^{TM}, were used to adjust the pH of the phenol solution for parametric studies under acidic and alkaline conditions. Phenol (C_6H_5OH) was obtained from HmbG Chemicals, and distilled water (H_2O) was used as the solvent throughout the experimental procedures.

2.2 Preparation of sodium alginate-iron (SA-Fe) solution

The sodium alginate and iron powder were weighed based on specific formulation ratios. Sodium alginate was first dissolved in 150 mL of distilled water and continuously stirred for 2 hours using a magnetic stirrer to ensure homogeneity. The solution was then allowed to rest at room temperature (25 ± 2°C) for 24 hours to fully hydrate the polymer chains. After 24 hours, the pre-weighed iron powder was gradually added to the SA solution under stirring and mixed for another 2 hours to ensure uniform dispersion. The resulting SA-Fe mixture was then allowed to rest for an additional 24 hours to stabilize the blend before bead formation.

2.3 Preparation of calcium chloride crosslinking solution

A 0.5 M calcium chloride solution was prepared by dissolving the required amount of $CaCl_2$ in distilled water and stored at room temperature. This solution served as the gelling medium for the sol-gel encapsulation process.

2.4 Fabrication of iron-based beads via sol-gel method

The iron-based beads were synthesized using the sol-gel droplet technique. A 25 mL syringe was filled with the prepared SA-Fe mixture. The solution was then carefully dripped, drop by drop, into a beaker containing the 0.5 M calcium chloride solution. As the droplets entered the solution, instantaneous ionic crosslinking occurred, forming spherical hydrogel beads. This process was repeated until all SA-Fe mixture was used. The beads were left in the $CaCl_2$ solution for 24 hours to ensure complete gelation, then filtered and rinsed with distilled water to remove excess ions.

2.5 Preparation of phenol stock and working solutions

A 10 ppm stock solution of phenol was prepared by dissolving 0.01 g of phenol in 1.0 L of distilled water under constant magnetic stirring. The pH of the solution was adjusted using 0.1 M HCl or 0.1 M NaOH to the desired value depending on the experimental condition (acidic, neutral, or alkaline). For photocatalytic testing, 50 mL

aliquots of this solution were used as working samples.

2.6 Characterization of catalyst beads

Fourier Transform Infrared Spectroscopy (FTIR) analysis was employed to identify the functional groups present in the fabricated iron beads and confirm the successful encapsulation of iron within the alginate matrix. The FTIR spectra were recorded in the wavelength range of 400–4000 cm^{-1}. The spectral data provided information on chemical bonding, metal–polymer interaction, and structural integrity of the beads.

2.7 Photocatalytic degradation procedure

The photocatalytic degradation experiments were carried out to assess the efficiency of the iron-based bead catalysts in removing phenol under various operating conditions. A phenol solution with a concentration of 10 ppm was prepared, and 100 mL of this solution was used for each test. The catalyst dosage was fixed at 30 g/L. Prior to irradiation, the mixture of the phenol solution and the iron bead catalyst was stirred in the dark for 2 hours to establish adsorption–desorption equilibrium between the catalyst surface and phenol molecules. This step was essential to differentiate between physical adsorption and actual photocatalytic degradation. Once equilibrium was achieved, the solution was exposed to visible light irradiation, and degradation performance was monitored for up to 3 hours. Samples were withdrawn at 15-minute intervals during the first hour and every 30 minutes thereafter. At each sampling point, 2.5 mL aliquots were collected, centrifuged to separate the catalyst, and analyzed using a UV–Visible spectrophotometer at 270 nm, corresponding to the characteristic absorbance peak of phenol.

2.8 Simple photoreactor setup

The photocatalytic reactions were conducted in a custom-designed batch photoreactor system. The system consisted of a UV fluorescent lamp with an emission range of 280–315 nm, positioned 15 cm above the reaction vessel. The reaction was carried out in 50 mL Pyrex conical flasks placed inside a light-sealed enclosure. To ensure uniform light distribution and minimize energy loss, the inner walls of the enclosure were lined with aluminum foil to enhance reflectivity. A magnetic stirrer was used to keep the catalyst particles suspended evenly throughout the solution, while a thermometer was used to continuously monitor the temperature and maintain stable ambient conditions during the photocatalytic reaction.

2.9 Determination of phenol concentration and degradation efficiency

Phenol concentration in the treated samples was determined using a UV-Vis spectrophotometer (UVmini-1240, Shimadzu) at 270 nm. The degradation efficiency of phenol was calculated using the equation below:

$$\text{Degradation } (\%) = \left(\frac{C0 - Ct}{C0}\right) \text{ x } 100 \quad (1)$$

Where, C_0 = initial concentration of phenol and C_t = concentration at time t

3. RESULTS AND DISCUSSION

3.1 Functional group determination

The functional groups present in the synthesized iron bead catalyst were identified using Fourier Transform Infrared (FTIR) spectroscopy, with spectral readings recorded in the range of 4000–400 cm^{-1}. FTIR analysis is essential to confirm the chemical bonding and functional integrity of the synthesized material, as it provides insights into the surface chemistry and interactions of the active sites. As illustrated in Figure 1, the FTIR spectrum of the iron bead catalyst exhibits a broad absorption band at 3446.96 cm^{-1}, corresponding to the stretching vibration of hydroxyl (–OH) groups, which may originate from adsorbed water or the alginate matrix. The band observed at 1638.11 cm^{-1} is attributed to the carbonyl (–C=O) stretching, indicating successful coordination between the iron nanoparticles and the alginate structure. Peaks at 1413.43 cm^{-1} and 1121.15 cm^{-1} are associated with the asymmetric and symmetric stretching vibrations of the carboxylate (COO^-) groups, respectively. The symmetric C–O vibration also appears prominently at 1121.15 cm^{-1}, reinforcing the presence of alginate functionalities. Most notably, a strong absorption band around 570.36 cm^{-1} confirms the presence of Fe–O stretching vibrations, which are characteristic of magnetite (Fe_3O_4) nanoparticles. This is further supported by the prominent band in the 500–700 cm^{-1} region, which is typically

associated with the stretching vibrations of Fe–O bonds in iron oxide structures [13,14]. These spectral features collectively confirm the successful incorporation of iron oxide within the bead matrix and validate the structural characteristics necessary for effective photocatalytic activity.

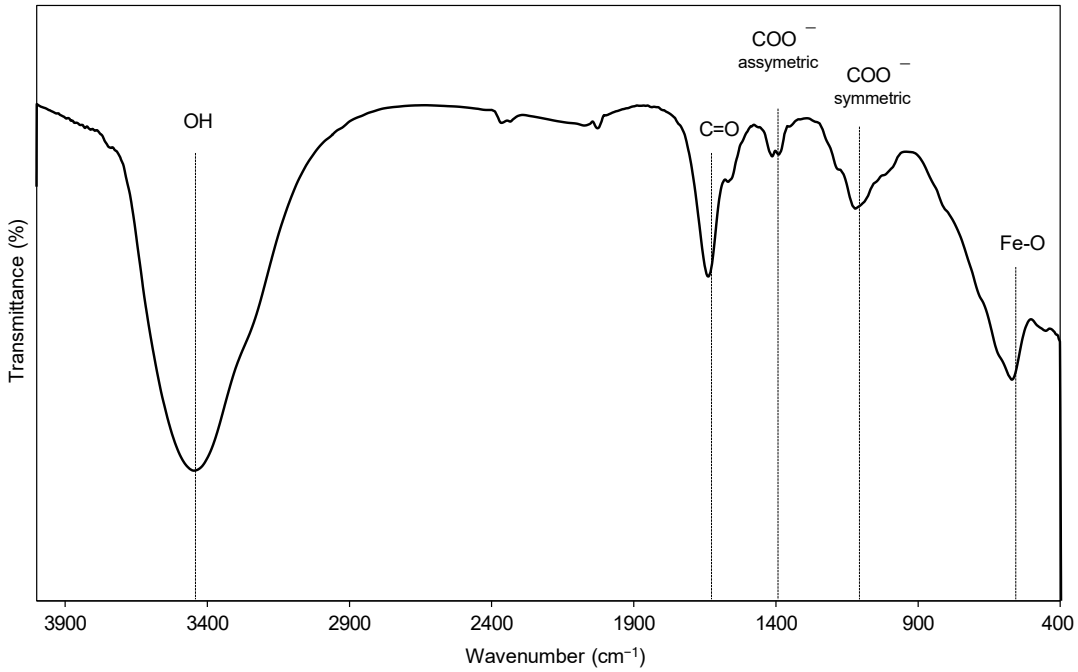

Fig. 1. FTIR spectrum of the synthesized iron-based bead catalyst showing characteristic functional group vibrations

3.2 Effect of pH

The photocatalytic performance of iron-based bead catalysts was significantly influenced by the pH of the solution. As illustrated in Figure 2, the highest phenol degradation efficiency was observed at pH 3, indicating that the catalyst performed best under acidic conditions. This trend can be attributed to the surface chemistry of magnetite nanoparticles; as pH increases, the surface of the nanoparticles becomes increasingly negatively charged, which enhances electrostatic repulsion between the catalyst and phenolate ions in solution [15]. Consequently, this repulsion diminishes the catalyst's ability to adsorb and degrade phenol molecules. Under acidic conditions, the phenol primarily exists in its neutral molecular form (below its pKa), which facilitates stronger interactions with the catalyst surface. As the pH shifts to more alkaline levels, phenol dissociates into negatively charged phenolate ions. These ions experience stronger electrostatic repulsion from the negatively charged surface of the iron bead, resulting in lower degradation efficiency [15]. Furthermore, the decrease in hydrogen bonding capability due to the electron-rich oxygen in phenolate ions may also contribute to reduced photocatalytic activity. Kumar et al. (2010) also reported that at higher pH values, increased electrostatic repulsion and reduced ionic mobility impair nanoparticle interaction with organic pollutants, further explaining the observed decline in performance [17].

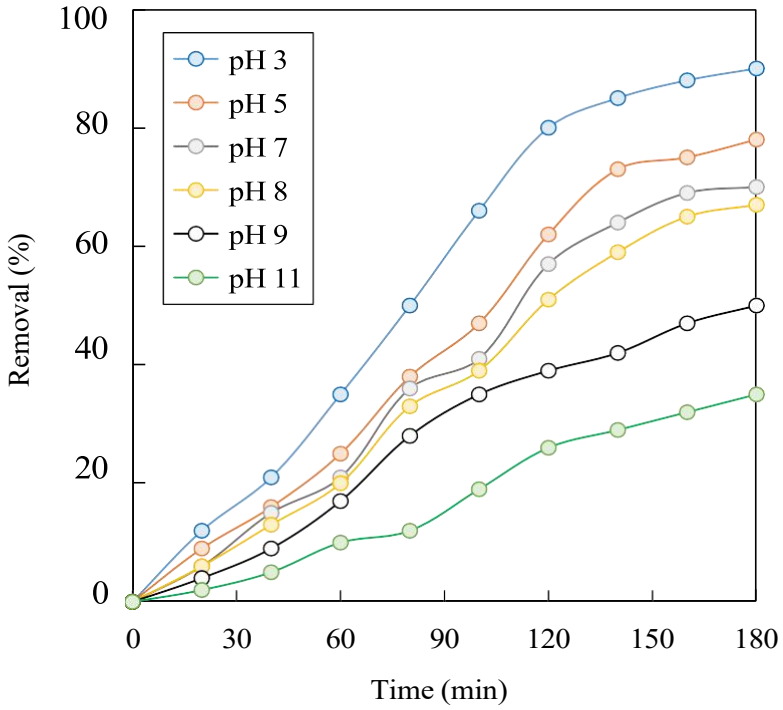

Fig. 2. Effect of pH on the photocatalytic degradation of phenol using iron bead catalyst [Catalyst dosage (W) = 30 g/L, Initial phenol concentration (C) = 10 ppm, Reaction time (t) = 3 h, Temperature (T) = 303.15 K]

3.3 Effect of catalyst dosage

Catalyst dosage plays a crucial role in determining the efficiency of the photocatalytic degradation process, as it directly influences the available surface area and the number of active sites for the reaction. As shown in Figure 3, increasing the dosage of iron bead catalyst from 10 g/L to 50 g/L resulted in a progressive enhancement of phenol removal efficiency. This is attributed to the greater surface area and higher concentration of active sites available to absorb photons and generate reactive species, thereby accelerating the degradation process. The removal efficiency increased in the following order: 10 g/L < 20 g/L < 30 g/L < 40 g/L < 50 g/L, confirming that higher catalyst loading promotes more efficient phenol degradation. However, a saturation point was observed at higher dosages (40 g/L and 50 g/L), where the degradation rate began to plateau. This suggests that the reaction reached an equilibrium state, where further increases in catalyst dosage did not significantly enhance performance. The phenomenon can be explained by the charge balance dynamics of ionic interactions within the system. According to Emmellin and Mahtab (2020), the equilibrium concentration of reacting ions is inversely related to the ionic strength within the reaction medium; thus, as the ionic charge density increases, the availability of reactants to sustain further degradation decreases [18]. Moreover, excessive catalyst dosages may lead to light scattering and shielding effects, reducing the penetration of light and thus the efficiency of photon utilization [19,20]. Therefore, while increasing catalyst dosage improves degradation efficiency up to a certain point, optimal dosage must be determined based on specific system parameters such as pollutant concentration and light intensity to avoid unnecessary material use and ensure cost-effective operation.

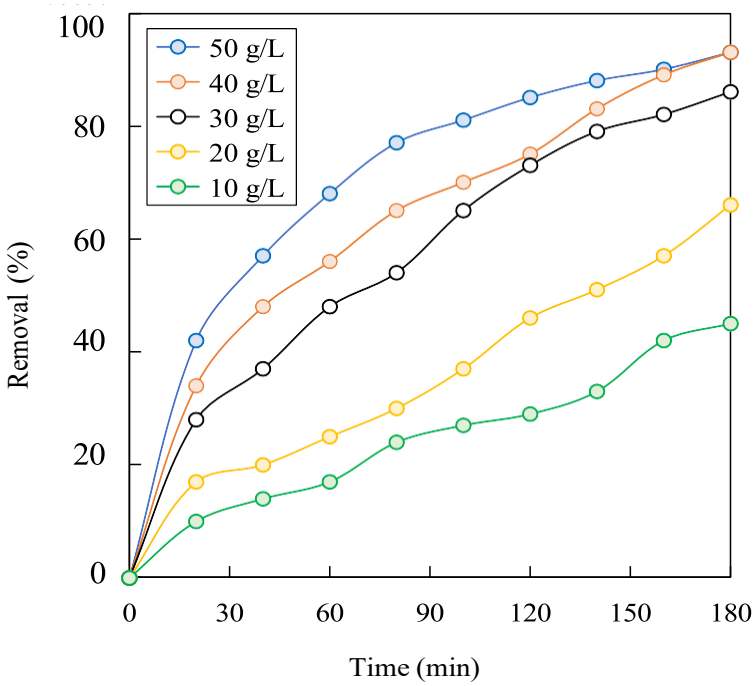

Fig. 3. Effect of catalyst dosage on phenol degradation using iron bead catalyst [pH = 3, Initial phenol concentration (C) = 10 ppm, Reaction time (t) = 3 h, Temperature (T) = 303.15 K]

3.4 Effect of initial concentration

The efficiency of photocatalytic degradation using iron bead catalysts is significantly influenced by the initial concentration of the phenolic compound. As shown in Figure 4, the degradation rate decreases as the initial phenol concentration increases from 10 ppm to 100 ppm. The highest degradation efficiency was observed at 10 ppm, followed by 20, 30, 40, 70, and 100 ppm, respectively. This inverse relationship is primarily due to the limited number of active sites on the catalyst surface relative to the increasing number of phenol molecules at higher concentrations. At lower concentrations, the available surface area of the iron bead catalyst is sufficient to adsorb and degrade phenol efficiently through both photocatalytic and adsorption mechanisms [21]. However, as the initial concentration increases, the excess phenol molecules compete for the same active sites, leading to surface saturation [22]. This competition reduces the efficiency of radical generation and subsequent degradation reactions. Moreover, at high concentrations, phenol molecules may block the catalyst surface, hindering light absorption and the formation of reactive oxygen species necessary for the photocatalytic process. Although iron is a commonly used and cost-effective catalyst, its photocatalytic activity is lower compared to high-activation-energy metals such as titanium or aluminum. This limitation becomes more pronounced at higher pollutant concentrations, where stronger oxidative power and larger surface areas are required. As highlighted by Arjunan and Karuppan (2013), the iron bead system operates via a heterogeneous mechanism combining both adsorption and degradation. For optimal performance in treating higher concentrations of phenol, catalyst dosage or surface area must be adjusted accordingly to maintain high degradation efficiency [23].

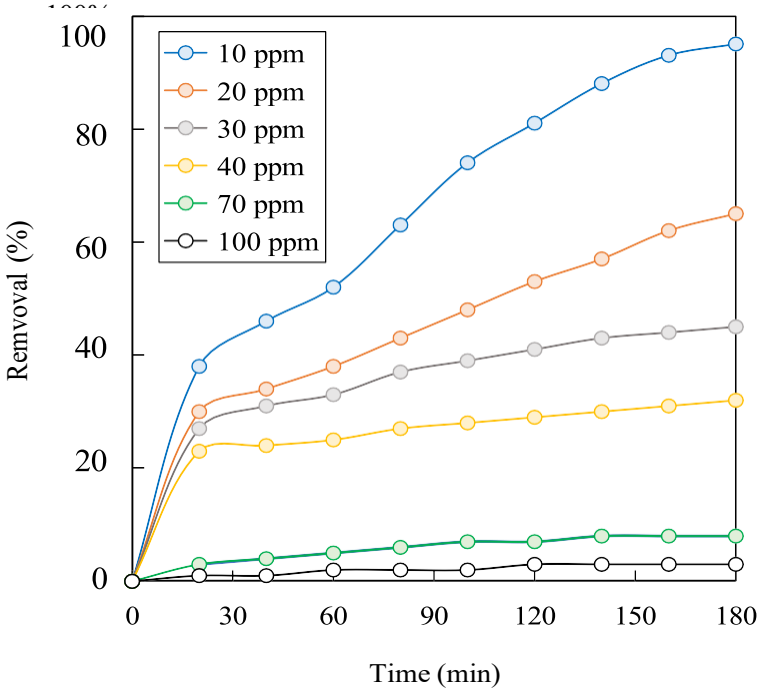

Fig. 4. Effect of initial phenol concentration on degradation using iron bead catalyst [pH = 3, Catalyst dosage (W) = 40 g/L, Reaction time (t) = 3 h, Temperature (T) = 303.15 K]

3.5 Comparison of catalyst performance

The performance evaluation, illustrated in Figure 5, was conducted to compare the photocatalytic degradation efficiency of the synthesized iron bead catalyst against its individual components; iron metal powder and alginate bead. For consistency, the same experimental parameters were applied to all three materials. The data for the iron bead catalyst was obtained from prior optimization studies, while the iron metal and alginate bead were tested separately under identical conditions. The results clearly demonstrate the superior performance of the synthesized iron bead catalyst compared to its individual counterparts. This performance gap highlights the synergistic effect achieved through the combination of iron and alginate in a structured bead form [24]. While iron metal alone exhibits relatively high ionic activity and can contribute to degradation reactions, its effectiveness is limited by its low surface area and susceptibility to hydrolysis in aqueous solutions, which reduces the number of reactive sites available for interaction with phenol molecules [7,11,12]. On the other hand, alginate beads formed through ionic cross-linking between sodium alginate and calcium chloride provide a stable matrix but exhibit weak photocatalytic activity. The ionic strength from calcium ions is significantly lower than that of transition metals like iron, resulting in limited generation of reactive species and slower degradation rates. By integrating iron into the alginate matrix through a sol-gel process, the resulting iron bead catalyst benefits from both the structural stability of alginate and the catalytic properties of iron. This combination not only increases the available surface area but also enhances charge mobility and facilitates effective interaction with light, thereby accelerating the degradation process [7,24].

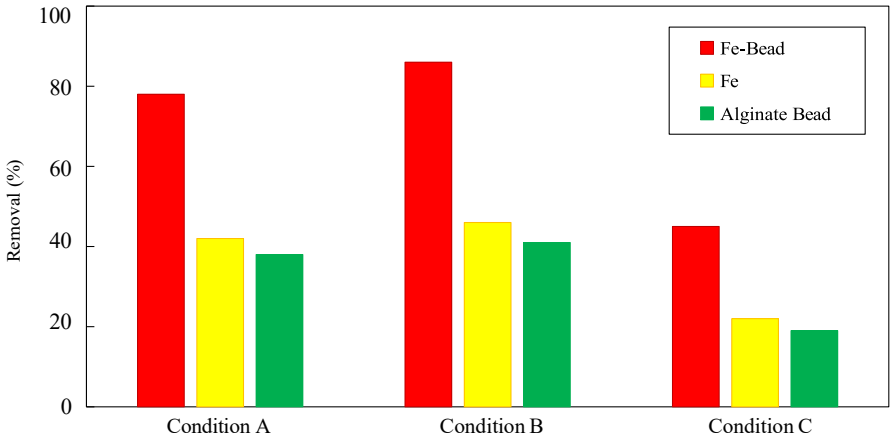

Fig. 5. Comparative performance study of iron-based bead catalysts under varying experimental conditions: (A = Alginate bead [pH = 5, catalyst dosage (W) = 30 g/L, phenol concentration (C) = 10 ppm, reaction time (t) = 3 h, temperature (T) = 303.15 K]; B = Iron powder [pH = 3, W = 30 g/L, C = 10 ppm, t = 3 h, T = 303.15 K]; C = Synthesized iron bead catalyst [pH = 3, W = 40 g/L, C = 30 ppm, t = 3 h, T = 303.15 K])

4. CONCLUSION

This study aimed to evaluate the photocatalytic degradation performance of synthesized iron-based beads toward phenol removal from aqueous solutions. Iron, a readily available and cost-effective metal, was selected due to its ability to generate and conduct ionic charges, which are essential for promoting redox reactions with phenolic compounds. The beads were synthesized using sodium alginate and iron powder via the sol-gel method, with calcium chloride serving as the crosslinking agent. The interaction between sodium alginate and calcium chloride formed a stable bead structure, while enhancing the ionic conductivity of the composite. This synergistic combination significantly improved the catalytic efficiency, nearly doubling the degradation performance compared to the individual components (iron or alginate alone). The photocatalytic activity of the synthesized iron beads was evaluated under varying parameters, including solution pH, catalyst dosage, and initial phenol concentration. The results revealed that phenol degradation was most effective under acidic conditions, with optimum performance observed at pH 3. Acidic pH favors greater availability of ionic charges, enhancing the interaction between the catalyst and phenol. Increasing the catalyst dosage improved degradation efficiency by providing a larger active surface area, although excess catalyst may lead to early equilibrium due to limited reactant availability. Conversely, higher initial phenol concentrations resulted in decreased degradation efficiency, likely due to surface saturation and blockage of active sites on the catalyst, which hindered the light-driven photocatalytic process. The photocatalytic degradation of phenol was found to be highly efficient under optimal conditions. At pH 3, with a catalyst dosage of 40 g/L, and a reaction time of 3 hours at 303.15 K, the system achieved up to 95% removal of phenol under visible light irradiation. These findings demonstrate the potential of iron-based beads as a cost-effective and efficient photocatalyst for the treatment of phenolic wastewater.

ACKNOWLEDGEMENT

The authors would like to express their sincere gratitude for the financial support from the Universiti Kuala Lumpur Branch Campus Malaysian Institute of Chemical and Bioengineering Technology (UniKL MICET) and Majlis Amanah Rakyat (MARA). Special thanks are also extended to Dr. Muhammad Farhan bin Hanafi for his valuable contributions as a UniKL Postdoctoral Researcher Fellow (UniKL/CoRI/Postdoc/1/12/24).

REFERENCES

1. Oladimeji, T. E., M. Oyedemia, M. E. Emetere, O. Agboola, J. B. Adeoye, and O. A. Odunlami. “Review on the Impact of Heavy Metals from Industrial Wastewater Effluent and Removal Technologies.” Heliyon 10 (2024): 1–30. https://doi.org/10.1016/j.heliyon.2024.e40370.

2. Yasir, N., A. S. Khan, M. A. Hassan, T. H. Ibrahim, M. I. Khamis, and P. Nancarrow. "Ionic Liquid Agar-Alginate Beads as a Sustainable Phenol Adsorbent." Polymers 14, no. 5 (2002): 984. https://doi.org/10.3390/polym14050984.
3. Hanafi, Muhammad Farhan, and Norzahir Sapawe. "A Review on the Water Problem Associated with Organic Pollutants Derived from Phenol, Methyl Orange, and Remazol Brilliant Blue Dyes." Materials Today: Proceedings 31, no. 1 (2021): A141–A150. https://doi.org/10.1016/j.matpr.2021.01.258.
4. Saltwork Technologies. "Removing Highly Toxic Phenolic Compounds." Wastewater Treatment Options, 2020. https://www.saltworkstech.com/articles.
5. Ingole, R. S., D. H. Lataye, and P. T. Dhorabe. "Adsorption of Phenol onto Banana Peels Activated Carbon." Journal of Civil Engineering 21, no. 1 (2018): 10–100. https://doi.org/10.1007/s12205-016-0101-9.
6. Hanafi, Muhammad Farhan, and Norzahir Sapawe. "A Review on the Current Techniques and Technologies of Organic Pollutants Removal from Water/Wastewater." Materials Today: Proceedings 31, no. 1 (2021): A158–A165. https://doi.org/10.1016/j.matpr.2021.01.265.
7. Hanafi, Muhammad Farhan, and Norzahir Sapawe. "An Overview of Recent Developments on Semiconductor Catalyst Synthesis and Modification Used in Photocatalytic Reaction." Materials Today: Proceedings 31, no. 1 (2021): A151–A157. https://doi.org/10.1016/j.matpr.2021.01.262.
8. Abdi, H., and J. Abedini. "MOF-Based Polymeric Nanocomposite Beads as an Efficient Adsorbent for Wastewater Treatment in Batch Continuous System: Modelling and Experiment." Chemical Engineering Journal 400 (2020): 4–16. https://doi.org/10.1016/j.cej.2020.125862.
9. Aziz, F., M. E. Achaby, A. Lisaneddine, K. Aziz, L. Ouzzani, R. Mamouni, and L. Mandi. "Composites with Alginate Beads: A Novel Design of Nano-Adsorbents Impregnation for Large-Scale Continuous Flow Wastewater Treatment Pilots." Saudi Journal of Biological Sciences 27, no. 10 (2019): 10–25. https://doi.org/10.1016/j.sjbs.2019.11.019.
10. Tong, K., Y. Zhang, and P. K. Chu. "Evaluation of Calcium Chloride for Synergistic Demulsification of Super Heavy Oil Wastewater." Colloids and Surfaces A: Physicochemical and Engineering Aspects 419 (2013): 46–52. https://doi.org/10.1016/j.colsurfa.2012.11.047.
11. Hanafi, Muhammad Farhan, and Norzahir Sapawe. "Enhanced Photocatalytic Degradation of Phenol Using Mesoporous Zinc Nanoparticles Catalyst." AIP Conference Proceedings 2923, no. 1 (2024): 040022. https://doi.org/10.1063/5.0195471.
12. Hanafi, Muhammad Farhan, Nazatulshima Hassan, and Norzahir Sapawe. "Performance Studies of TiO_2 Catalyst for Phenol Degradation." Materials Science Forum 1076 (2022): 215–220. https://doi.org/10.4028/p-mu9929.
13. Das, A. K., A. Marwal, and R. Verma. "Bio-Reductive Synthesis and Characterization of Plant Protein Coated Magnetite Nanoparticles." Journal of Nano Hybrids 7 (2014): 69–86. https://doi.org/10.4028/www.scientific.net/NH.7.69.
14. Wu, S., A. Sun, F. Zhai, J. Wang, W. Xu, Q. Zhang, and A. A. Volinsky. "Fe_3O_4 Magnetic Nanoparticles Synthesis from Tailings by Ultrasonic Chemical Co-Precipitation." Materials Letters 65 (2011): 1882–1884. https://doi.org/10.1016/j.matlet.2011.03.065.
15. Chiang, Y. J., and C. C. Lin. "Photocatalytic Decolorization of Methylene Blue in Aqueous Solutions Using Coupled ZnO/SnO_2 Photocatalysts." Powder Technology 246 (2013): 137–143. https://doi.org/10.1016/j.powtec.2013.04.033.
16. AbdoJlahi, K., F. Yazdani, R. Panahi, and B. Mokhtarani. "Biotransformation of Phenol in Synthetic Wastewater Using the Functionalized Magnetic Nano-Biocatalyst Particles Carrying Tyrosinase." 3 Biotech 8 (2018): 419. https://doi.org/10.1007/s13205-018-1445-2.
17. Kumar, N. S., M. Suguna, M. V. Subbaiah, A. S. Reddy, N. P. Kumar, and A. Krishnaiah. "Adsorption of Phenolic Compounds from Aqueous Solutions onto Chitosan-Coated Perlite Beads as Biosorbent." Industrial & Engineering Chemistry Research 49, no. 19 (2010): 9238–9247. https://doi.org/10.1021/ie901171b.
18. Emmellin, T., and D. Mahtab. "Common-Ion Effect in Solubility Equilibria." LibreTexts, 2020, 23–407.
19. Abdel-Wahab, A. M., A. S. Al-Shirbini, O. Mohamed, and O. Nasr. "Photocatalytic Degradation of Paracetamol over Magnetic Flower-like TiO_2/Fe_2O_3 Core–Shell Nanostructures." Journal of Photochemistry and Photobiology A: Chemistry 347 (2017): 186–198. https://doi.org/10.1016/j.jphotochem.2017.07.030.
20. Akpan, U. G., and B. H. Hameed. "The Advancements in Sol–Gel Method of Doped-TiO_2 Photocatalysts." Applied Catalysis A: General 375 (2010): 1–11. https://doi.org/10.1016/j.apcata.2009.12.023.
21. Khaki, M. R. D., M. S. Shafeeyan, A. A. A. Raman, and W. M. A. W. Daud. "Application of Doped Photocatalysts for Organic Pollutant Degradation: A Review." Journal of Environmental Management 198 (2017): 78–94. https://doi.org/10.1016/j.jenvman.2017.04.099.
22. Lin, J. C. T., M. D. G. Luna, G. L. Aranzamendez, and M. C. Lu. "Degradations of Acetaminophen via a $K_2S_2O_8$-Doped TiO_2 Photocatalyst under Visible Light Irradiation." Chemosphere 155 (2016): 388–394. https://doi.org/10.1016/j.chemosphere.2016.04.059.
23. Arjunan, B., and M. Karuppan. "Treatment of Phenol-Containing Wastewater by Photoelectron-Fenton Method Using Supported Nanoscale Zero-Valent Iron." Environmental Science and Pollution Research 20, no. 3 (2013): 1596–1605. https://doi.org/10.1007/s11356-012-0990-1.
24. Zamanhuri, Norezatul Shahiral Ahmad, Norzahir Sapawe, Muhammad Farhan Hanafi, Siti Fatimah Ibrahim, Lusi Ernawati, Bernard Maringgal, and Daniel Joe Dailin. "Ni-Nanoparticle Beads: An Advanced Nano-Catalyst for Efficient Photocatalytic Degradation of Pharmaceuticals." Journal of Advanced Research in Micro and Nano Engineering 36, no. 1 (2025): 1–11. https://doi.org/10.37934/armne.36.1.111.